



G&G

Micro-World

Editor: Nathan Renfro

Contributing Editors: John I. Koivula and Tyler Smith

Breyite in Diamond

The author recently examined a 0.71 ct, D-color, type IaB diamond with an interesting inclusion reminiscent of a stone splashing in water (figure 1). Raman analysis identified the well-formed colorless transparent crystal as breyite (CaSiO_3), a calcium-rich silicate mineral commonly found in sublithospheric or superdeep diamonds. It was hypothesized that this diamond formed in the lower part of the transition zone or the lower mantle beneath the earth's crust.

Since the majority of diamonds in the jewelry industry come from the lithosphere, each one provides a window into Earth's intricate geology. Inclusions such as this one serve as a reminder that beauty and flaws may coexist peacefully, whether they add to a diamond's charm or provide scientific insight.

Aprisara Semapongpan
GIA, Bangkok

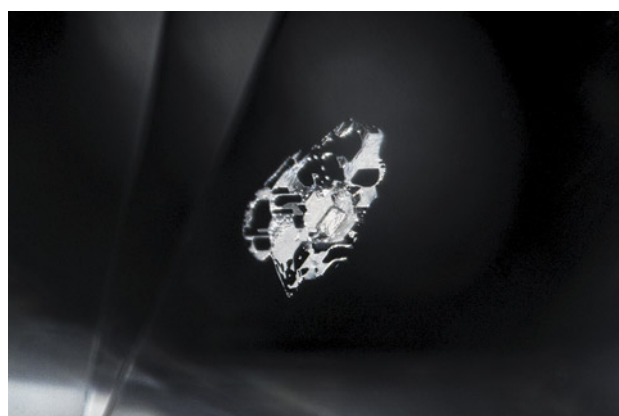


Figure 1. A well-formed colorless breyite crystal reminiscent of a stone making a splash in water. Photomicrograph by Aprisara Semapongpan; field of view 1.07 mm.

Spray of Columbite Crystals in Topaz

A probable columbite inclusion in beryl was featured in a recent Quarterly Crystal, demonstrating the striking

form these minerals can display (Spring 2023 *G&G Micro-World*, pp. 90–91). It was only fitting to follow up with a look at the same inclusion hosted by a different mineral.

The cluster of bladed columbite crystals in figure 2, identified via Raman spectroscopy, was found in an 8.91 ct colorless topaz. The thinner crystals allowed the brown bodycolor to show through, while the thicker, sword-like center crystal appeared black and opaque. Thin-film interference was observed between the host and inclusion when illuminated with oblique lighting, adding some welcome color to an otherwise featureless crystal face. While columbite has been previously described in topaz (Fall 2009 *G&G*

About the banner: Numerous epidote crystals show colorful birefringence in plane-polarized light within their rock crystal quartz host. Photomicrograph by Nathan Renfro; field of view 5.75 mm.

GEMS & GEMOLOGY, VOL. 59, NO. 3, pp. 370–379.

© 2023 Gemological Institute of America

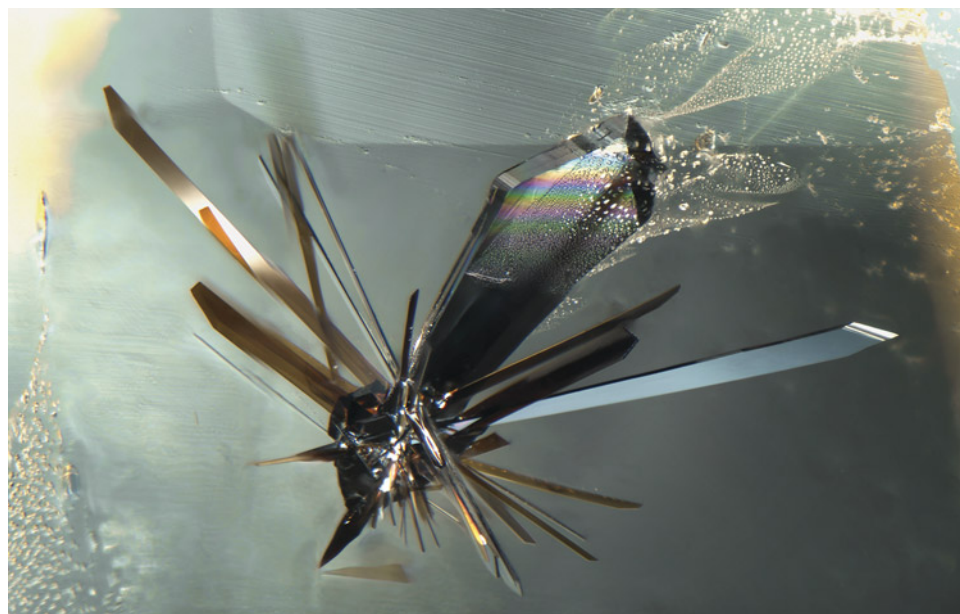


Figure 2. Bladed crystals of columbite radiate from a central point in colorless topaz. The mirror-like surfaces allow for reflections of neighboring blades, as seen in the top left crystal. Photomicrograph by Tyler Smith; field of view 2.90 mm.

Lab Notes, pp. 212–213; E.J. Gübelin and J.I. Koivula, *Photoatlas of Inclusions in Gemstones, Volume 2*, Opinio Publishers, Basel, Switzerland, 2005, pp. 263, 738), this is the most dramatic example observed by the author.

Tyler Smith
GIA, New York

Inclusion Resembling a Gada in Diamond

Recently, the authors observed an interesting etch channel (figure 3) in a 1.00 ct L-color type Ia round brilliant diamond with SI₁ clarity. It resembled a *gada*, a mace-like

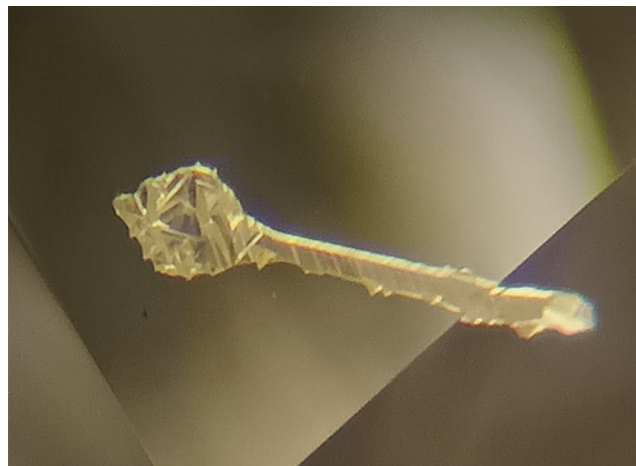
weapon belonging to the Hindu god Hanuman. This etch channel was the only one observed in the diamond; these features are often created by dissolution processes (T. Lu et al., "Observation of etch channels in several natural diamonds," *Diamond and Related Materials*, Vol. 10, No. 1, 2001, pp. 68–75).

This unusual clarity characteristic showcases the variety that is possible within the natural world.

Rujal Kapadia and Bhavya Maniar
GIA, Surat

Sally Eaton-Magaña
GIA, Carlsbad

Figure 3. This etch channel seen in the crown facets of a 1.00 ct diamond with SI₁ clarity (left) resembled a gada (right), a mace-like weapon wielded by the Hindu god Hanuman. Photomicrograph (left) by Deepak Raj; field of view 0.80 mm. Photo (right) courtesy of the Metropolitan Museum of Art.



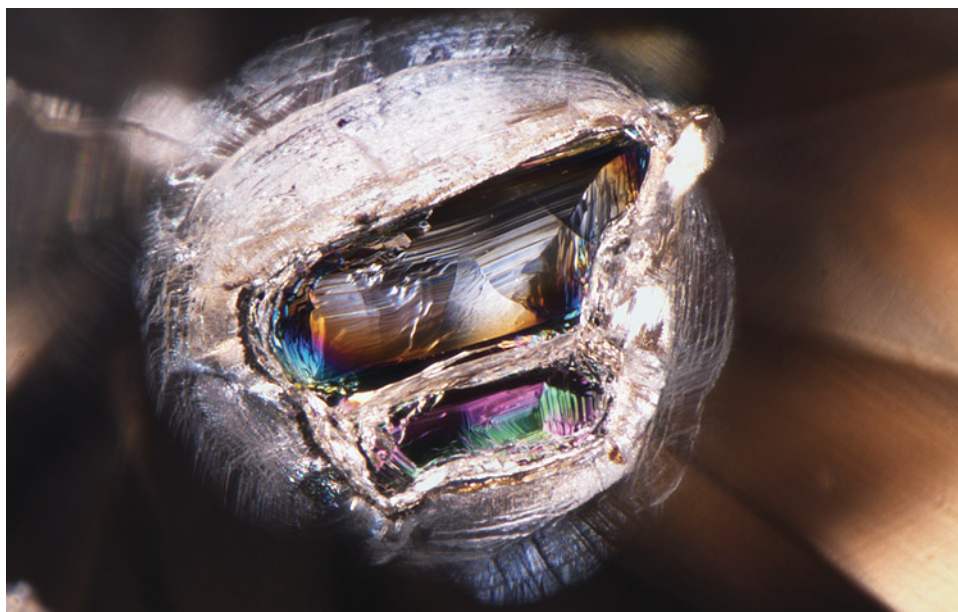


Figure 4. This iridescent ferropericlasite crystal with a stress halo measuring approximately 0.7 mm was trapped inside a light brown diamond. Photomicrograph by Kyaw Soe Moe; field of view 1.58 mm.

Iridescent Inclusion in Brown Diamond

The iridescent crystal inclusion in the 1.07 ct light brown type IIa diamond in figure 4 was identified by Raman spectroscopy as ferropericlasite. Ferropericlasite, $(\text{Mg,Fe})\text{O}$, can originate from either shallow (lithospheric) or deep (sublithospheric) depths within the earth. A stress halo was developed around the crystal by temperature and pressure changes during the ascent to the earth's surface. The colorful iridescence may have been caused by light interference at a thin film trapped between the inclusion and the host diamond. It is rare to see ferropericlasite as an inclusion in diamond, especially such a large crystal.

*Kyaw Soe Moe
GIA, New York*

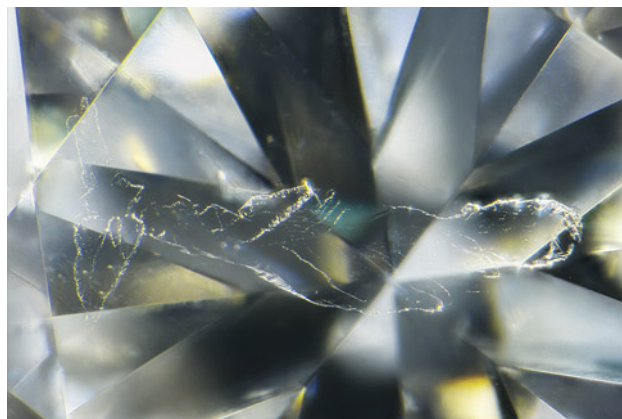
Natural Diamond with Twinning Wisps Resembling a Whale

The authors recently examined a 0.46 ct type Ia round brilliant diamond with SI₁ clarity that had surprisingly patterned twinning wisps. When viewed through the table, the twinning wisps resembled a whale (figure 5). Twin planes can form in diamond when the orientation of the crystal structure changes during growth in the earth's mantle. Twinning wisps are atomic defects along this plane, found in ~10% of type Ia diamonds (S. Eaton-Magaña et al., "Natural-color D-to-Z diamonds: A crystal-clear perspective," Fall 2020 *G&G*, pp. 318–335).

A termination of one of these features just below the pavilion was examined using photoluminescence (PL) mapping at various excitation wavelengths to examine the distribution of atomic-level defects in the crystal lattice. The PL mapping with 455 nm excitation revealed a relative increase in the defect concentrations of the nitrogen-related centers of H3 (NVN⁰) with zero-phonon line (ZPL)

at 503.2 nm and H4 (4N+2V) with ZPL at 495.9 nm; a weak radiation-related defect, the TR12 with ZPL at 469.9 nm was also detected (A.M. Zaitsev, *Optical Properties of Diamond*, Springer-Verlag, Berlin and Heidelberg, 2001, and references therein). PL mapping using 633 nm excitation revealed that the GR1 (V⁰; ZPL at 741.2 nm) had a higher Raman-normalized peak area corresponding to the termination of the twinning wisp compared to diamond adjacent to the wisp. The GR1 defect is typically formed by radiation damage of a diamond lattice. Although the GR1 was elevated, we did not observe radiation stains around the twinning wisps. Furthermore, there were no visible changes to the color of the diamond's fluorescence when exposed to deep ultraviolet luminescence, which can occur with significant radiation exposure.

Figure 5. This round brilliant diamond displays twinning wisps that resemble a whale. Photomicrograph by Nathan Renfro; field of view 2.62 mm.



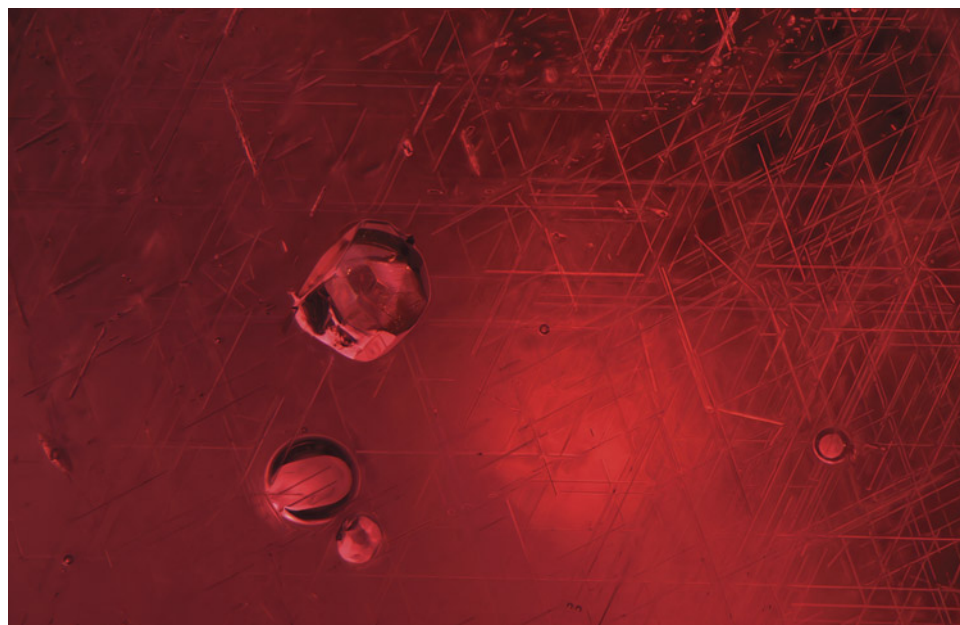


Figure 6. Gas bubbles hide just beneath natural crystal inclusions in this garnet and glass doublet. Photomicrograph by Emily Jones; field of view 1.58 mm.

This stone offers an example of how natural growth processes in diamond can result in microscopic features that occasionally form delightful patterns.

Taryn Linzmeyer and Roy Bassoo
GIA, Carlsbad
Jaldeep Sojitra
GIA, Surat

A Red Herring in a Red Garnet

At first glance, a 2.54 ct round mixed-cut stone examined by the author presented itself as a natural red garnet. Microscopic inspection revealed a host of transparent crystals and widespread epitaxial needles, both typical inclusions for garnet. Upon closer inspection, however, some of the apparent “crystals” were recognized as gas bubbles, betrayed by their smooth spherical forms (figure 6). This distinction can be easily missed without careful examination under high magnification. Additional observations and testing conclusively identified the material as pyrope-almandine garnet fused with manufactured glass. As with most garnet-topped doublets, the garnet portion was cut to occupy the crown while the glass made up most of the pavilion so that the natural inclusions of the garnet top masked the telltale signs of manufactured glass beneath.

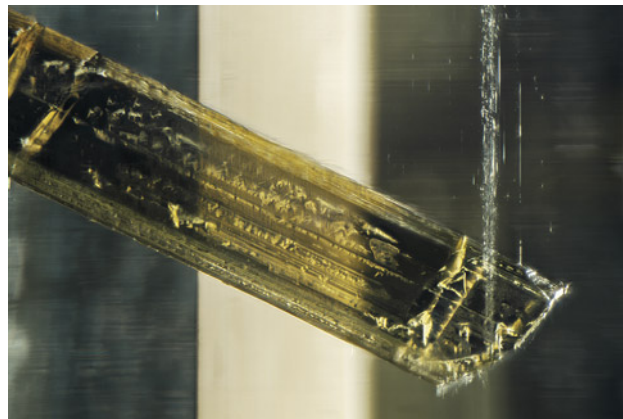
Emily Jones
GIA, New York

Heliodor with a Large Schorl Inclusion

An 8.33 ct long rectangular heliodor, the yellow variety of beryl (ideally $\text{Be}_3\text{Al}_2\text{Si}_6\text{O}_{18}$), was examined by the author. It was reportedly from the Zelatoya Vada mine in Murgab, Tajikistan; however, it was likely from Pakistan (J.S.

White, “Let’s get it right: Tajikistan heliodor,” *Rocks and Minerals*, Vol. 80, No. 4, 2005, pp. 285–286). The heliodor had a large schorl tourmaline inclusion prominently under the table facet (figure 7) and a small schorl tourmaline near one corner. A thin band of fine fluid inclusions ran parallel to the length of the stone adjacent to the tourmaline. The stone was clearly cut to highlight the interesting inclusion rather than hide or remove it; aside from the two tourmaline inclusions and the thin band of fluids, the beryl had high clarity.

Figure 7. Morphological features of the tourmaline crystal included in the heliodor are visible; striations and triangular growth marks are present. A band of fluid inclusions is visible near the tip of the schorl tourmaline. Photomicrograph by Rhiana Elizabeth Henry; field of view 2.90 mm. Gift of Mark Mauthner, GIA Museum no. 37772.



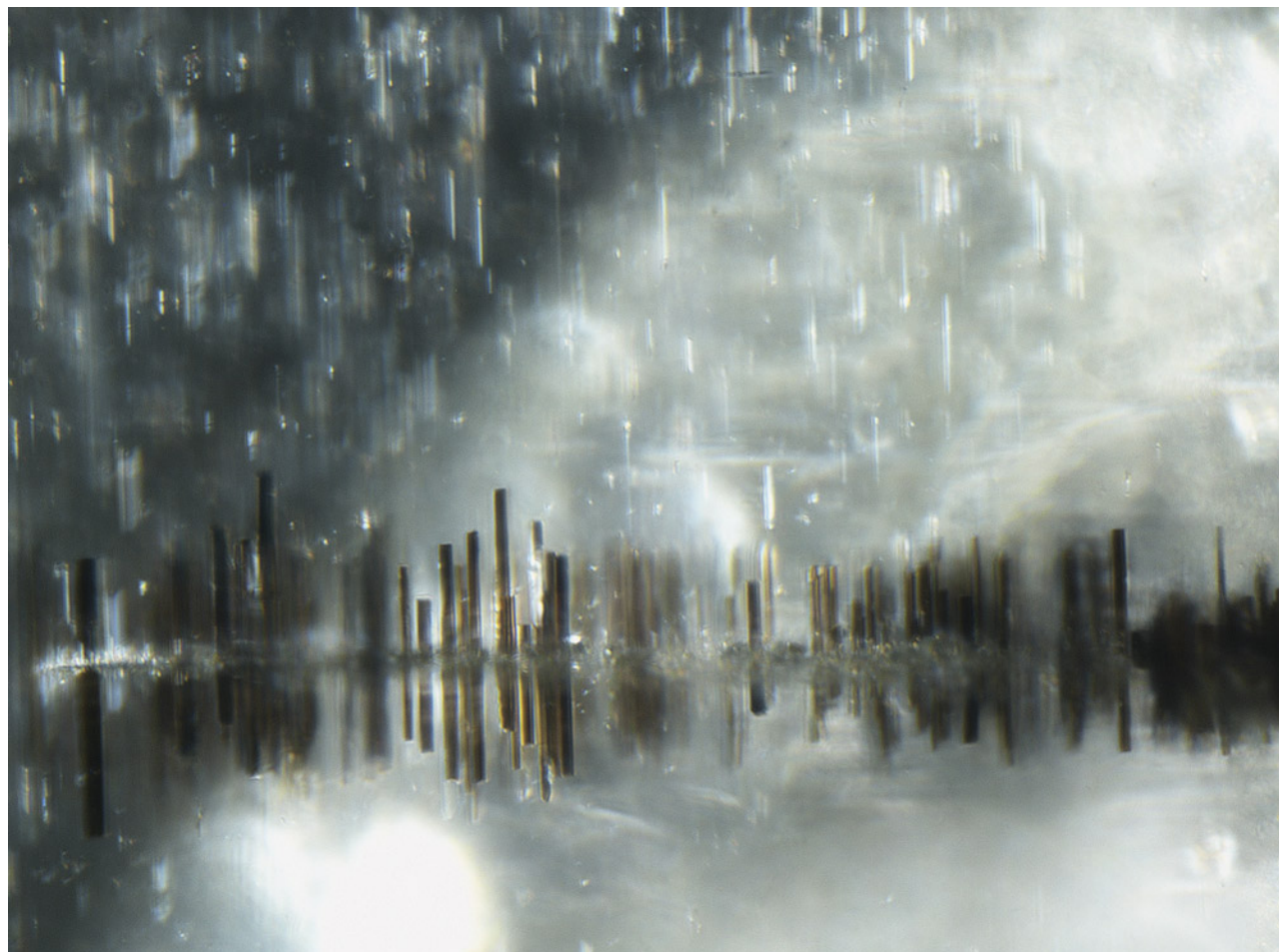


Figure 8. Blade-like magnetite inclusions developed from a healed fracture in a 2.08 ct Burmese peridot resemble a rainy lakeside city. Photomicrograph by Makoto Miura; field of view 1.06 mm.

Both the heliodor and the tourmaline were analyzed by Raman spectroscopy and laser ablation–inductively coupled plasma–mass spectrometry (LA-ICP-MS) to better understand the structure and chemistry of the minerals. Analyses were conducted on the girdle of the heliodor and on the back end of the tourmaline inclusion where it intersected a pavilion facet. The heliodor had low-moderate water bound in its structural channels, as determined qualitatively by Raman spectroscopy, which is expected for heliodor with low sodium content (R.E. Henry et al., “Crystal-chemical observations and the relation between sodium and H₂O in different beryl varieties,” *Canadian Mineralogist*, Vol. 60, No. 4, 2022, pp. 625–675). The heliodor fit well within the expected chemistry; it had low overall cation substitutions, with minor or trace iron, magnesium, lithium, sodium, and cesium content. The tourmaline was confirmed to be schorl dominant due to its predominant sodium and iron content; however, due to high vacancy at the X structural site, the tourmaline had a high foitite component (D.J. Henry et al.,

“Nomenclature of the tourmaline-supergroup minerals,” *American Mineralogist*, Vol. 96, 2011, pp. 895–913).

After data collection for research, this stone will be used in the GIA GemKids program as an educational piece for young students at the Carlsbad campus. It will represent the heliodor variety of beryl, showing fascinating inclusions as well as evidence of LA-ICP-MS laser pits on the girdle of the stone (not shown in the photomicrograph).

Rhiana Elizabeth Henry
GIA, Carlsbad

Rainy Lakeside City in Peridot

Inclusions in gemstones provide useful information regarding their geological origin. A 2.08 ct Burmese peridot containing unique black blade-like inclusions developed from healed fractures (fingerprints), as shown in figure 8. Raman spectroscopy identified these blade-like inclusions as magnetite. Tiny raindrop-like magnetite lamellae were also ob-

served throughout the stone. Such inclusions in Burmese peridot sometimes create four-rayed asterism. According to previous studies, the presence of magnetite lamellae suggests the oxidation or dehydration of olivine by geological processes. This image resembles a rainy lakeside city landscape.

*Makoto Miura
GIA, Tokyo*

ural healing process of a fracture oriented parallel to the *c*-axis.

These zigzag-patterned fingerprints often indicate a Sri Lankan origin, but they can also be found in sapphires from Myanmar and Madagascar. The undamaged rectilinear pattern could indicate that the stone is unheated.

*Yuxiao Li
GIA, Tokyo*

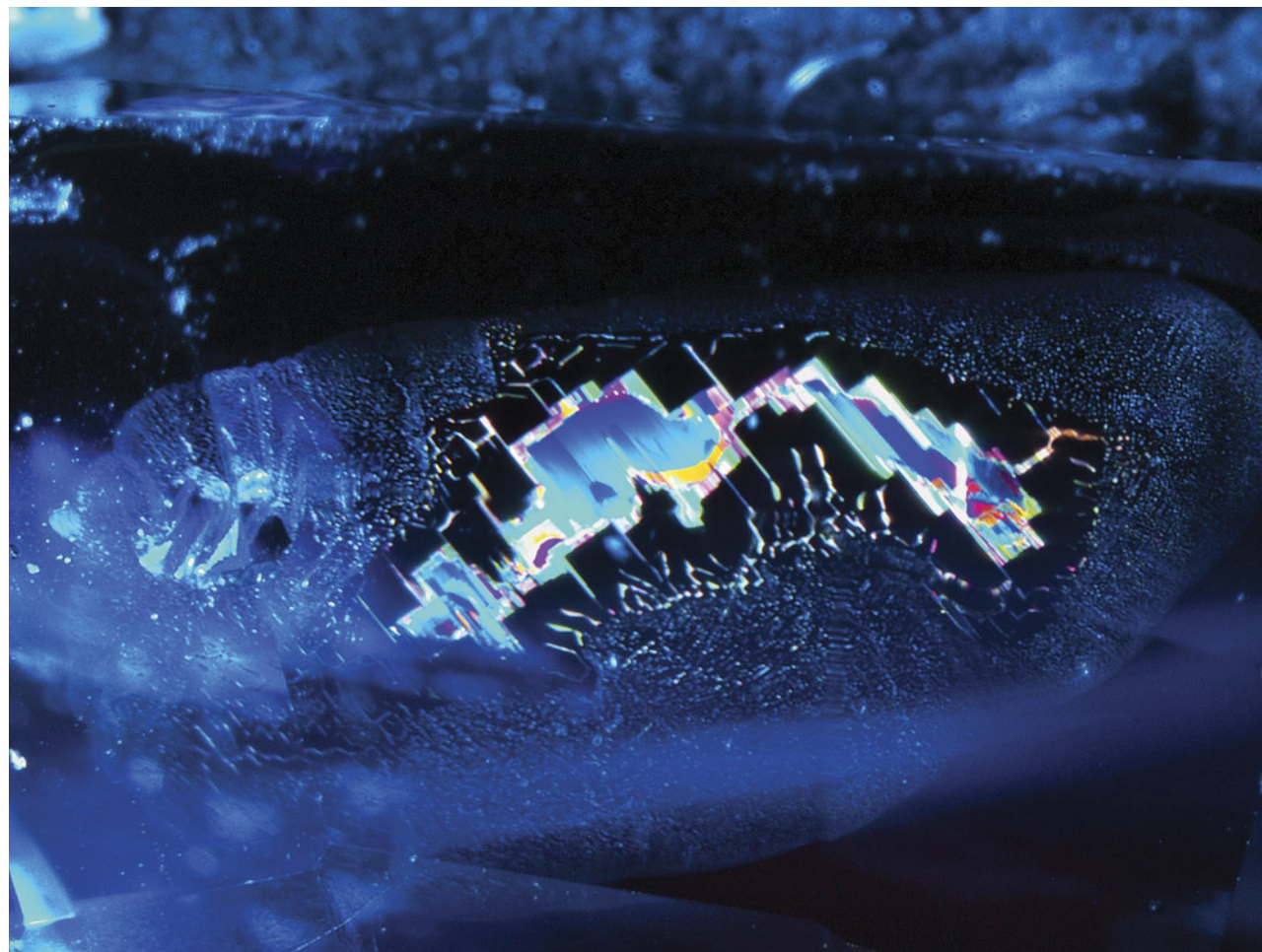
Zigzag Fingerprint in Sri Lankan Sapphire

The author recently examined a 3.21 ct oval mixed-cut blue sapphire. Chemical analysis and gemological observation of internal fissures suggested a Sri Lankan origin. Under fiber-optic illumination, the fingerprints showed rectilinear zigzag-patterned films with vibrant colors that resulted from thin-film interference (figure 9). The rectilinear structure of this fingerprint was caused by the nat-

Fissure with Moiré Pattern in Spinel

Surface-reaching fissures commonly host precipitates of epigenetic minerals, as was the case with a 4.22 ct purple spinel recently examined by the author. "Islands" of unidentified birefringent inclusions occupied a near-planar fissure. These inclusions were inert to Raman spectroscopy. Delicate depositions radiating from these islands interacted to create a complex moiré pattern (figure 10).

Figure 9. The rectilinear zigzag-patterned fingerprint in this 3.21 ct blue sapphire shows beautiful vibrant colors, indicating a Sri Lankan origin. Photomicrograph by Yuxiao Li; field of view 4.45 mm.



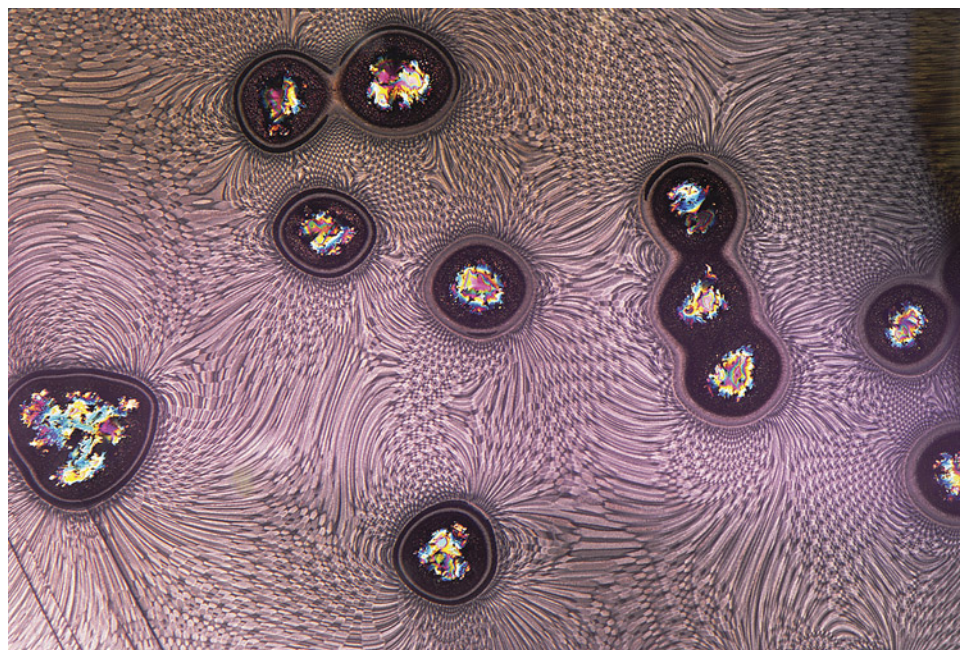


Figure 10. A precipitation of an unidentified mineral in a fissure of a purple spinel creates this highly intricate moiré pattern. A combination of oblique fiber-optic and darkfield illumination was used. Photomicrograph by Tyler Smith; field of view 2.90 mm.

Moiré patterns, named after their resemblance to a type of fabric, form when parallel or concentric lines overlap. It is unclear whether the islands formed first and were partially dissolved in a secondary event, or if they formed simultaneously with the spinel. Although moiré patterns have been observed in partially healed fluid fingerprints and surface-reaching fissures, it is rare to see them expressed in such a spectacular form.

Tyler Smith

Large Stellate Dislocation in Spinel

The author recently examined a 4.49 ct greenish blue spinel exhibiting a prominent stellate inclusion characterized by a network of needle-like dislocations clustered in a six-rayed star pattern (figure 11). The inclusion was large enough to be readily observed without magnification.

Star-like needles have been previously documented in spinel originating from Vietnam. These findings contribute to our understanding of spinel and its origins, providing

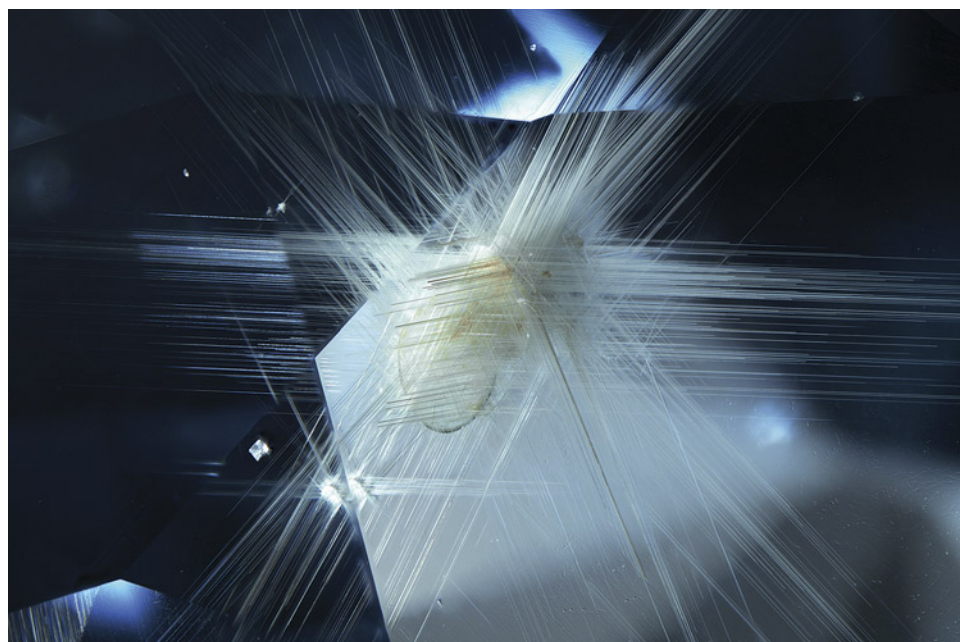


Figure 11. Stellate dislocations decorate the interior of a greenish blue spinel believed to be from Vietnam. Photomicrograph by Ezgi Kiyak; field of view 4.79 mm.

valuable information for gemologists. This is one of the most remarkable stellate inclusions the author has observed in a spinel.

*Ezgi Kiyak
GIA, New York*

Tourmaline in Emerald

The author recently examined a 3.80 ct emerald with well-formed black, opaque prismatic crystals (figure 12). The surface-reaching crystals were identified as tourmaline through the use of Raman spectroscopy. While tourmaline crystals are relatively uncommon inclusions, they have been documented in emeralds from Zambia, Pakistan, Russia, and Ethiopia, all of which are schist-hosted deposits. Laser ablation–inductively coupled plasma–mass spectrometry chemical analysis combined with inclusion observation revealed this emerald to be of Zambian origin.

*Virginia Schneider
GIA, New York*

Turquoise Planet Earth

Armenia is not a widely known source of turquoise, but a recent donation to GIA's colored stone reference collection proved that the country can produce high-quality, aesthetically pleasing stones. One of them, cleverly cut into an

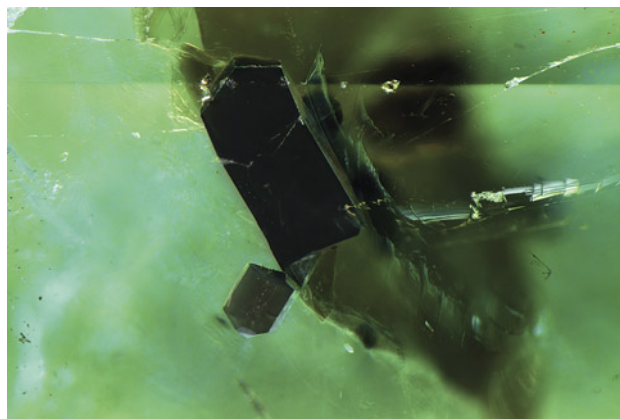


Figure 12. Prismatic black tourmaline in a Zambian emerald. Photomicrograph by Virginia Schneider; field of view 1.76 mm.

84.90 ct sphere measuring $23.70 \times 23.88 \times 23.91$ mm, bore an astonishing resemblance to planet Earth (figure 13). The natural brown matrix material mimicked the continents, while the greenish blue turquoise represented the oceans. Infrared spectroscopy showed that, like most gem turquoise, the specimen had been polymer impregnated, a treatment that makes the stone more durable. Additionally,

Figure 13. An 84.90 ct sphere of Armenian turquoise measuring $23.70 \times 23.88 \times 23.91$ mm displays a striking resemblance to planet Earth. Left: Diffuse fiber-optic lighting allows the face of the stone to be seen in full. Right: Pinpoint fiber-optic lighting creates an appearance of day and night cast onto Earth. Gifted to GIA's colored stone reference collection by Gemfab CJSC. Photos by Britni LeCroy.

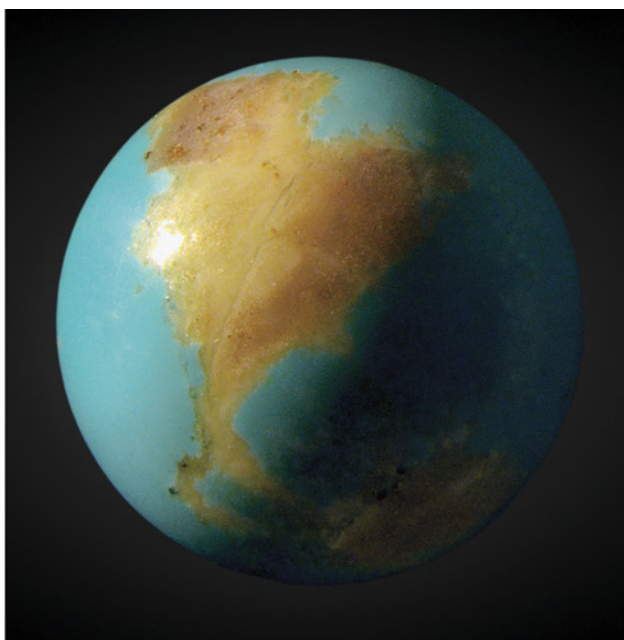
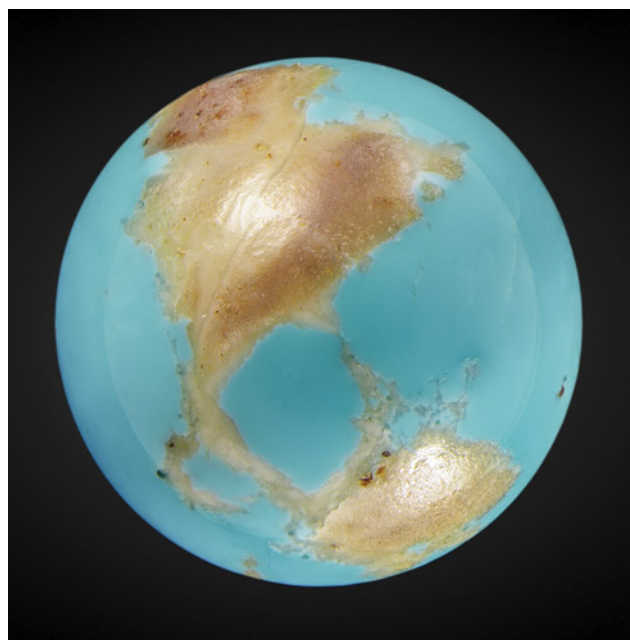




Figure 14. Dark yellowish to brownish green needle-like inclusions dominate the interior of this 21.36 ct Portuguese fluorapatite on siderite matrix. Photo by Adriana Robinson.

no dye was detected. To accentuate its likeness to our planet, the sphere was photographed against “Musou Black,” marketed as the world’s blackest fabric and advertised to absorb 99.905% of all light. Precise placements of

pinpoint lighting created various appearances of a sunlit Earth suspended in space.

*Britni LeCroy
GIA, Carlsbad*

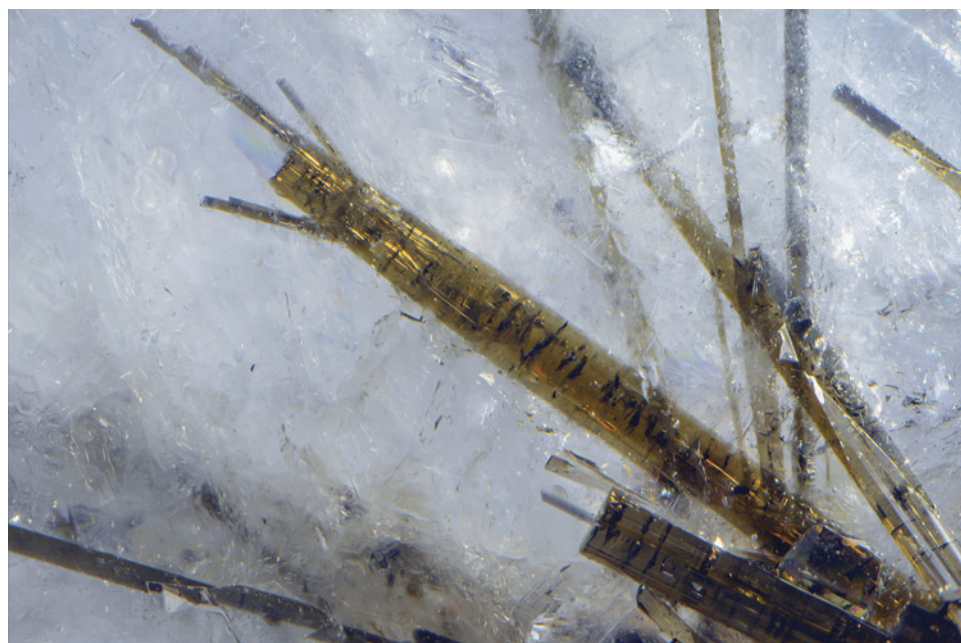


Figure 15. Raman analysis was used to identify the acicular inclusions in the fluorapatite host crystal as dravite tourmaline. Photomicrograph by Nathan Renfro; field of view 7.37 mm.

Quarterly Crystal: Dravite in Fluorapatite

Growing from an angular matrix plate of brown siderite, a doubly terminated hexagonal crystal weighing 21.36 ct with a very light purplish blue color (figure 14) was identified as fluorapatite by Raman analysis. As the photo shows, the semitransparent crystal clearly hosts a number of randomly arranged, eye-visible, translucent acicular inclusions. The fluorapatite thumbnail specimen, from the Panasqueira mine in the Castelo Branco district of Covilhã, Portugal, was acquired by author JIK from the col-

lection of Dr. Vasco Trancoso at auction in June 2023. When the specimen was examined microscopically, the acicular morphology and dark yellowish to brownish green bodycolor of the inclusions, as well as their behavior in polarized light, suggested they might be tourmaline. Laser Raman microspectrometry was able to pinpoint their identity as dravite (figure 15), a member of the tourmaline group.

*John I. Koivula, Nathan Renfro, and Maxwell Hain
GIA, Carlsbad*

